Orientational ordering in mixed cyanide crystals: $(NaCN)_{1-x}(KCN)_x$

Ailan Cheng and Michael L. Klein
Department of Chemistry and Laboratory for Research on the Structure of Matter, University of Pennsylvania, Philadelphia, Pennsylvania 19104-6323

Laurent J. Lewis
Département de Physique et Groupe de Recherche en Couches Minces, Université de Montréal, Case Postale 6128, Succursale A, Montréal, Québec, Canada H3C 3J7

(Received 13 December 1990)

The technique of constant-pressure molecular dynamics is used to investigate the influence of random strain fields on the structure of solid $(NaCN)_{1-x}(KCN)_x$ mixtures at two concentrations in the orientational-glass-forming range, namely $x=0.50$ and 0.85. The simulations reveal that Na^+ ions act as nucleation centers that lock neighboring CN^- ions into one of six equivalent $\langle 100 \rangle$ orientations, with the C end preferentially pointing towards Na^+. In the $x=0.5$ mixture, CN^- ions favor $\langle 100 \rangle$ orientations at all temperatures studied. At the lower Na^+ concentration, $x=0.85$, Na^+ lock most neighboring anions into $\langle 100 \rangle$ directions at a relatively high temperature. Upon further cooling, however, overall freezing into $\langle 111 \rangle$ orientations dominates. The competition between these two freezing-in processes leads to an anomalous temperature dependence of the orientational-order parameters for CN^- at low Na^+ concentration.

I. INTRODUCTION

At high temperatures, the pure cyanides RbCN, KCN, and NaCN are cubic crystals (space group $Fm3m$), in which CN^- ions undergo rotational diffusion. As the temperature decreases, long-wavelength transverse acoustic phonons undergo a tremendous softening. This phenomenon is a precursor to the first-order structural phase transition from cubic to orthorhombic (space group $Immm$) that takes place at 288 K for NaCN and at 168 K for KCN. Further cooling results in an antiferroelectric transition at 172 K for NaCN and 83 K for KCN.[1-5]

Two distinct types of cyanide mixtures result from the substitution of either cations or anions by another ionic species. In mixtures of alkali cyanide with an alkali halide, $(MX)_{1-x}(MCN)_x$, where M is an alkali metal and X a halogen, an orientational glass forms at low temperature for cyanide concentrations below a critical value x_c. Here, CN^- ions do not order cooperatively but rather freeze into random orientations due to the presence of random strain fields. Substitution of one type of cation by another, such as $(RbCN)_{1-x}(KCN)_x$ and $(NaCN)_{1-x}(KCN)_x$, however, leads to very different behavior,[6-8] although the process also gives rise to random strain fields for CN^- ions. In $(RbCN)_{1-x}(KCN)_x$, for instance, the first-order transition is observed over the whole concentration range because the size difference between two cations ($r_{Rb^+}=1.48$ Å and $r_{K^+}=1.33$ Å) is not large enough to destroy the long-range orientational order, although the transition temperatures are reduced significantly from a linear interpolation between the values for pure RbCN and KCN. In $(NaCN)_{1-x}(KCN)_x$, however, the size disparity is large ($r_{Na^+}=0.98$ Å and $r_{K^+}=1.33$ Å), and the first-order transition is only observed in the vicinity of the pure phases. In the latter system, the CN^- ions freeze into random orientations at low temperature in the concentration range between the two critical concentrations $x_{c_1}=0.15$ and $x_{c_2}=0.9$.[6,9-11]

A variety of experimental techniques[12] such as Brillouin scattering,[13,14] dielectric relaxation,[1,9,10] neutron diffraction,[6,11,15-20] NMR,[21] Raman scattering,[22] torsion pendulum,[23] ultrasonic attenuation,[7,8,24-27] and x-ray diffraction,[28,29] have been used to investigate the phase diagram of mixed-cyanide crystals. There have also been numerous theoretical studies.[30-37] The main thrust of this work is in the characterization of the low-temperature orientational glass phase.

The measured shear elastic constant c_{44} has a very distinctive dependence on composition.[6,8,14,23] At concentrations close to either pure KCN or pure NaCN, c_{44} changes dramatically with temperature, while in the middle of the concentration range ($0.3<x<0.6$), c_{44} varies only very slowly with temperature.[8] The room-temperature neutron-diffraction data[20] suggest that, in the $x=0.44$ and 0.59 mixtures, CN^- ions have a strong preference for $\langle 100 \rangle$ orientations, while there appears to be a combination of $\langle 100 \rangle$ and $\langle 111 \rangle$ ordering in the $(NaCN)_{0.15}(KCN)_{0.85}$ mixture.

Here, we present the results of a computer-simulation study of $(NaCN)_{1-x}(KCN)_x$ mixtures at two concentrations, namely $x=0.5$ and 0.85. The simulation shows that Na^+ ions act as nucleation centers which lock neighboring CN^- ions into $\langle 100 \rangle$ directions; the remaining anions, i.e., those that do not have at least one Na^+ nearest neighbor, freeze into $\langle 111 \rangle$ orientations. For the $x=0.5$ mixture, where virtually all CN^- have at least

one Na^+ neighbor, $\langle 100 \rangle$ orientations are therefore favored at all temperatures; this observation agrees well with neutron-scattering experiments. For the $x=0.85$ mixture, on the other hand, the anion orientations shift from $\langle 100 \rangle$ to $\langle 111 \rangle$ as the temperature drops, reflecting the competition between these two freezing mechanisms, and causing the low-temperature orientational order parameters to exhibit an anomalous temperature dependence. This latter prediction has yet to be tested by experiment.

II. DETAILS OF THE CALCULATIONS

A. Molecular dynamics

The molecular-dynamics (MD) calculations have been performed under conditions of constant pressure.[38–43] This allows changes in both volume and shape of the simulation cell to take place in response to changing external conditions—in this case the temperature; the technique is particularly well suited to the study of structural transformations. Simulations were carried out at a number of temperatures through the molecular orientation freezing transition, i.e., in the range 300–50 K. The simulation cell consisted of $4\times4\times4$ unit cells, and thus contained 256 cations and an equal number of anions. Potassium and sodium ions were distributed at random on the cation sublattice.

The model potentials were taken from previous studies of the alkali cyanides.[44–48] Atom-atom Buckingham pair potentials with a real-space cutoff of 11 Å, were used. The usual combining rules were employed for the cross pairs. The relevant parameters are listed in the Table I.

The CN^- ion was taken to be rigid with a bond length of 1.17 Å. The charge distribution was described by an array of three fractional charges: $-0.8e$ on the N atom, $+0.8e$ on the C—N bond between C and N, and $-1.0e$ close to the C atom, but outside the C—N bond. The orientations of CN^- ions are influenced by both short-range atom-atom and long-range electrostatic interactions, and the latter depends sensitively on the charge distribution. A systematic study[47] of the problem concluded that no single model could work well for all alkali cyanides, but modest adjustments of the charge distribution for different crystals could produce rather satisfactory results. For example, CN^- ions in KCN have more "free volume" than in NaCN, and the model should reflect this fact. With this in mind, the CN^- charge distributions for $(NaCN)_{1-x}(KCN)_x$ mixtures were obtained by linear interpolation between those fitted for pure KCN and NaCN. The actual charge models used for the two concentrations we have investigated are listed in Table II. The electrostatic interactions were treated by the Ewald summation method,[49] using a cutoff in reciprocal space of 1.9 $Å^{-1}$ and a damping factor $\kappa=0.3$ $Å^{-1}$.

TABLE I. Parameters for the Buckingham potentials. The potentials are of the form $U_{\alpha\beta}=A_{\alpha\beta}\exp(-c_{\alpha\beta}r)-B_{\alpha\beta}r^{-6}$. The usual combining rules are used for the cross interactions, namely, $A_{\alpha\beta}=(A_{\alpha\alpha}A_{\beta\beta})^{1/2}$, $B_{\alpha\beta}=(B_{\alpha\alpha}B_{\beta\beta})^{1/2}$, and $c_{\alpha\beta}=(c_{\alpha\alpha}+c_{\beta\beta})/2$.

$\alpha\beta$	A (kJ mol^{-1})	c (Å^{-1})	B (Å^6 kJ mol^{-1})
Na-Na	40 900	3.155	101
K-K	151 000	2.967	1 464
C-C	174 300	3.400	2 569
N-N	192 000	3.600	1 718

The Parrinello-Rahman equations of motion for the translational degrees of freedom were integrated using a third-order Gear predictor-corrector algorithm.[50] The rotational degrees of freedom, expressed in terms of quarternions, were solved with a fourth-order Gear algorithm. The initial MD configurations were set up as fcc lattices (NaCl structure), with random orientations assigned to the CN^- molecules. The initial lattice constants were determined as follows: Since the potential model used does not lead to exactly the same lattice constant as experiment, the system was allowed to relax under zero pressure in order to release the excess pressure due to the model. The simulation was then restarted with the new lattice constant and zero external pressure. The high-temperature samples were cooled down gradually. At each temperature, the first 3000 time steps (of 2×10^{-15} s each) were discarded, then 4000 (sometimes 6000) time steps were collected for subsequent statistical analysis.

B. Orientational ordering

The main focus of this work is on anion orientational behavior. The orientation of a CN^- molecular ion is described in terms of an orientational distribution function $f(\hat{u})$, where $\hat{u}=(x,y,z)$ is the unit vector along the C—N bond. $f(\hat{u})$ can be developed into the Kubic-harmonics expansion[51]

$$4\pi f(\hat{u})=1+C_4K_4+C_6K_6+\cdots, \tag{2.1}$$

where

$$C_4=\langle K_4\rangle=(\tfrac{21}{16})^{1/2}\langle[5(x^4+y^4+z^4)-3]\rangle, \tag{2.2}$$

$$C_6=\langle K_6\rangle =(\tfrac{13}{128})^{1/2}\langle[21(x^4+y^4+z^4)+462x^2y^2z^2-17]\rangle. \tag{2.3}$$

For perfect $\langle 111 \rangle$ orientations, $C_4=-1.527$ and $C_6=2.266$, while $C_4=2.290$ and $C_6=1.275$ for $\langle 100 \rangle$ ordering. For free rotors, C_4 and C_6 approach zero. These coefficients are of particular interest since they can be estimated from neutron scattering and NMR experiments.[2,21]

The orientational freezing process can also be monitored in terms of the order parameters introduced by Ed-

TABLE II. Discrete charge model for the CN^- ion. Distances d are measured from the center of mass; the charge $-0.8e$ is located exactly on the N atom.

x	$d(-0.8e)$ (Å)	$d(0.8e)$ (Å)	$d(-1.0e)$(Å)
0.50	0.54	−0.445 85	−0.867 85
0.85	0.54	−0.431 89	−0.856 70

wards and Anderson in the study of spin glasses.[52] Thus, dipole order is described by three functions of T_{1u} symmetry,

$$Y_1^{(1)}=(3/4\pi)^{1/2}x, \tag{2.4}$$

$$Y_2^{(1)}=(3/4\pi)^{1/2}y\ , \tag{2.5}$$

$$Y_3^{(1)}=(3/4\pi)^{1/2}z\ , \tag{2.6}$$

whereas quadrupolar order is described by two functions of E_g symmetry,

$$Y_1^{(2)}=(15/16\pi)^{1/2}(3z^2-1)\ , \tag{2.7}$$

$$Y_2^{(2)}=(15/16\pi)^{1/2}(x^2-y^2)\ , \tag{2.8}$$

and three functions of T_{2g} symmetry,

$$Y_3^{(2)}=(15/4\pi)^{1/2}xy\ , \tag{2.9}$$

$$Y_4^{(2)}=(15/4\pi)^{1/2}yz\ , \tag{2.10}$$

$$Y_5^{(2)}=(15/4\pi)^{1/2}xz\ . \tag{2.11}$$

The order parameters $[\langle Y(\hat{u})\rangle]_{\rm av}$ and $([\langle Y(\hat{u})\rangle^2]_{\rm av})^{1/2}$ are calculated in the course of the simulations. In the above, $\langle\cdots\rangle$ denotes the time average for an individual CN^- ion, and $[\cdots]_{\rm av}$ the system average (i.e., over all ions).

III. SIMULATION RESULTS

A. $x=0.5$ mixture

A series of simulations were carried out for the $x=0.5$ mixture to study the evolution of the CN^- orientations as a function of temperature and, in particular, the formation of the orientational glass phase. Thermodynamic properties, such as the total potential energy and the volume of the MD cell, were evaluated and are given in Table III. The simulation cell is characterized by three vectors, **a**, **b**, and **c**, determined by the edge lengths of the simulation box, a, b, and c, together with the three angles between them, α, β, and γ. The temperature dependences of these six parameters are shown in Fig. 1. (The unit-cell lengths, L_a, L_b, and L_c, are obtained from the MD cell lengths by dividing by 4.) On average, the lattice is clearly cubic at room temperature. Upon cooling, the cell parameters stay approximately equal, although small deviations can be observed at the lowest temperature (less than 0.5% for the cell lengths). The small deviations seen in Fig. 1 are likely due to the finite size of the system, and especially to the fact that the K^+ and Na^+ spatial distributions are not perfectly isotropic. In particular, the orientations of the CN^- ions depend strongly on the cation distribution (this point will be discussed in detail later), and the CN^- orientations, in turn, influence the displacement of cations and anions, therefore causing small distortions of the simulation cell.

Although the lattice remains approximately cubic, the low-temperature pair-correlation functions for Na-Na, Na-K, and K-K, displayed in Fig. 2, reveal that Na^+ ions are displaced from the average cubic sites. The average displacement is approximately 2% of the mean lattice constant. In the mixture, the smaller Na^+ cations have more space to move, which, in turn, results in a broader Na-Na nearest-neighbor peak, and a leading edge at a shorter distance. Indeed, the first K-K peak is much sharper. Nonsystematic deviations are observed for second neighbors. The Na-Na second peak occurs at a smaller distance than the corresponding K-K one. However, the Na-K peak lies outside the K-K peak and corresponds to a separation larger than the 6.18 Å, average lattice parameter (recall Fig. 1). For cation pairs further apart, the local random distortions more or less average out as strong random strain fields destroy the long-range correlations. Such short-range distortions of the cation sublattice do not appear to have been observed experimentally.

TABLE III. Thermodynamic properties of the $x=0.5$ mixture. $\langle U_{\rm conf}\rangle$ and $\langle V\rangle$ are the run-averaged configurational energy and volume, respectively.

T (K)	$\langle U_{\rm conf}\rangle$ (kJ mol^{-1})	$\langle V\rangle$ (Å^3)
50.8	−728.97	233.77
88.3	−727.61	234.72
109.9	−726.75	235.50
132.1	−725.82	236.01
152.1	−724.86	236.53
170.5	−724.17	237.05
251.4	−720.85	239.85
310.0	−718.65	242.14

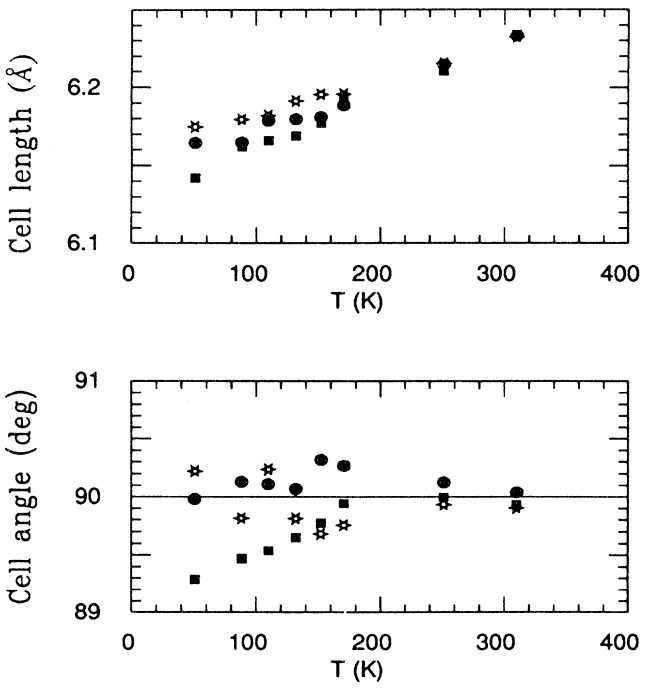

FIG. 1. Temperature dependence of the lengths of the three unit-cell vectors (L_a, L_b, L_c) and angles (α, β, γ) for the $x=0.50$ mixture. L_a, L_b, and L_c have been scaled to coincide with the high-temperature fcc lattice constant.

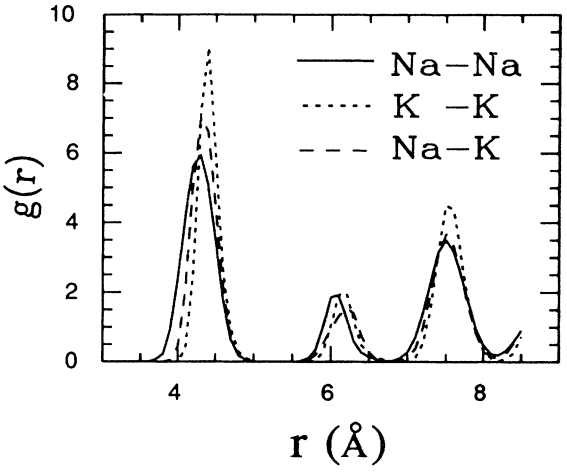

FIG. 2. Cation pair-distribution functions $g(r)$ for the $(NaCN)_{0.5}(KCN)_{0.5}$ mixture at 50 K. Solid line: Na-Na; dotted line: K-K; dashed line: Na-K.

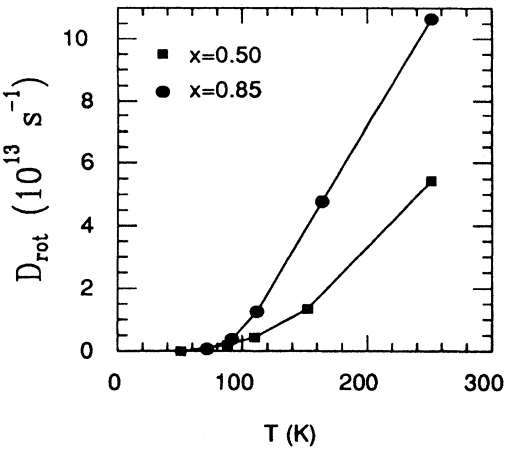

FIG. 4. Temperature dependence of the CN^- ion rotational diffusion constants D_{rot} for $x = 0.50$ (squares) and 0.85 (circles).

The first two Kubic-harmonics coefficients are shown in Fig. 3. Even above room temperature, as indicated by the large positive value of C_4, anions have a strong preference for ⟨100⟩ orientations. This result is in agreement with experimental data.[20] In fact, anions remain in either of the six ⟨100⟩ directions at all temperatures in this system, as inferred from the gradual increase of C_4 as temperature decreases. On the time scale of the simulation, the CN^- orientations are completely frozen along ⟨100⟩ directions at ~70 K; this can be seen from the temperature dependence of the rotational diffusion constants, shown in Fig. 4.

The Edwards-Anderson order parameters are shown in Fig. 5. The average values of the quantities $[\langle Y(\hat{u})\rangle]_{av}$ are almost zero, indicating that the net dipole moment of the system is small. The values of $([\langle Y(\hat{u})\rangle^2]_{av})^{1/2}$ indicate that T_{2g} quadrupolar order is weaker than that of E_g symmetry at all temperatures, in agreement with our earlier findings that ⟨100⟩ orientations are favored. As temperature decreases, the order parameters correspondingly increase.

In order to gain insight into the nature of the low-temperature phase, we examine time-averaged (over 8 ps) configurations. For the MD cell used in the present study, there are eight distinct atomic planes perpendicular to each axis. Four out of the eight planes along the z axis are displayed in Fig. 6. Here, the positions of all cations, as well as the center of masses and orientations of all CN^- ions are plotted. It is immediately evident from these plots that C atoms prefer the proximity of Na^+ ions, while N atoms prefer K^+. The pair-distribution functions for Na-C and Na-N correlations, plotted in Fig. 7, support this picture quantitatively. The first nearest-

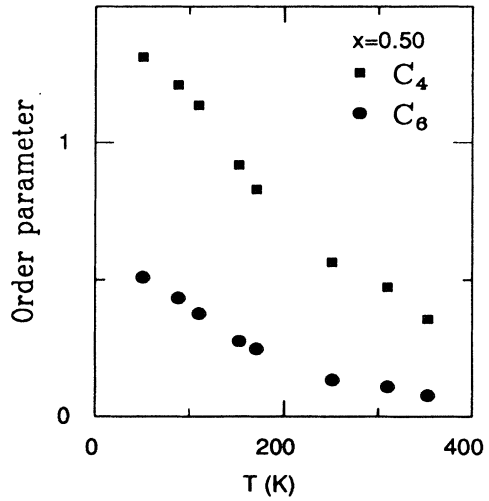

FIG. 3. Temperature dependence of the first two coefficients, C_4 and C_6, in the Kubic-harmonics expansion of the orientational distribution function $f(\hat{u})$, for the $(NaCN)_{0.5}(KCN)_{0.5}$ mixture.

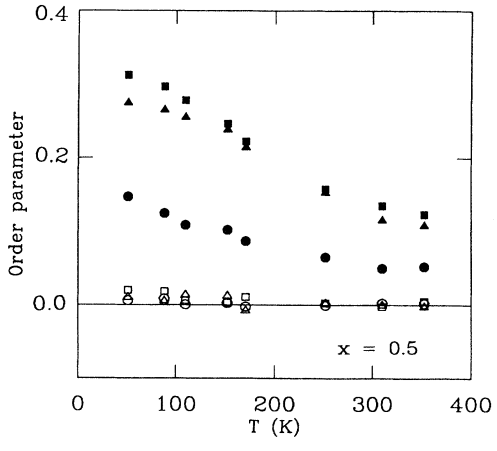

FIG. 5. Temperature dependence of order parameters for the $x = 0.5$ mixture. Open and solid symbols correspond, respectively, to $[\langle Y(\hat{u})\rangle]_{av}$ and $([\langle Y(\hat{u})\rangle^2]_{av})^{1/2}$: triangles, $Y_{T_{1u}}(\hat{u})$; squares, $Y_{E_g}(\hat{u})$; and circles, $Y_{T_{2g}}(\hat{u})$.

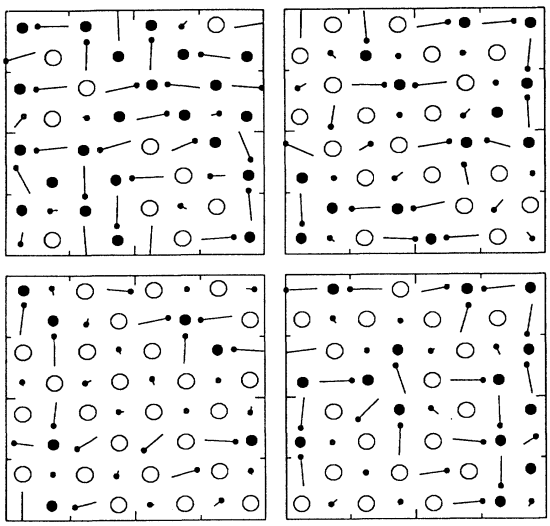

FIG. 6. Time-averaged configurations for four {001} atomic planes taken from the simulation for the $x=0.5$ mixture at 50 K. The position of each cation, and center of mass and orientation of each CN^- ion, are shown: large solid circles: Na^+; open circle: K^+; small solid circles: C; solid line: C-N bond. ⟨100⟩ orientations are clearly favored.

neighbor Na-C peak is sharper and positioned at a smaller r value than that for Na-N pairs. However, the first K-N peak occurs at smaller separation than the corresponding K-C peak. This feature can be understood in terms of the CN^- charge model discussed earlier. The stronger electrostatic field produced by the smaller cation, Na^+, favors the electronegative C end of the anion. However, the effective diameter of carbon used in the simulation is about 3% larger than that of nitrogen. It therefore also reduces the local strain in the lattice if C rather than N atoms pair with Na^+. When taking into account the small size disparity (3%) between C and N atoms, but the large difference in charge (20%), electrostatic interactions dominate the energetics of the system, even though "packing arguments" also play an important role in determining the orientations of the CN^- ions.

Probability distributions, denoted $\rho(\langle \hat{u}_i \cdot \hat{u}_j \rangle)$, which characterize the correlation of bond-vector directions for successively more distant pairs of CN^- molecules, are shown in Fig. 8 for the system at 90 K. The distributions are essentially independent of anion separation, an observation which indicates the presence of a strong "lock-in" effect that has destroyed long-range orientational order. The substantial portion of the molecules that align perpendicular to one another ($\cos\theta_{ij}=0$) likely prevents the lattice from distorting, and also results in weaker T_{2g} ordering compared with E_g (recall Fig. 5). This more rigid arrangement of the anions leads to a relatively weak temperature dependence of the shear elastic constant c_{44}, shown in Fig. 9. Here, c_{44} was calculated by evaluating the sound velocity from the period of oscillation of the intermediate scattering function, $F(Q,t)$.[45,47] The calculated values are about 30% higher than the corresponding experimental numbers,[6,8,14,23] in part because of the quite different frequency (time) scales associated with the measurements and the simulations.

It is clear from the above discussion that the anion orientations are largely determined by the spatial distributions of the cations. Although some CN^- ions are locked into ⟨100⟩ directions, and librate within only a small solid angle about their equilibrium positions at low temperature, lack of long-range correlations make it impossible to have a spatial-periodicity of anion orientations.

B. $x=0.85$ mixture

Results for the potential energy and the volume of the simulation cell as a function of temperature for the mixture $(NaCN)_{0.15}(KCN)_{0.85}$ listed in Table IV indicate that both quantities change smoothly upon cooling. The corresponding cell parameters are shown in Fig. 10. While

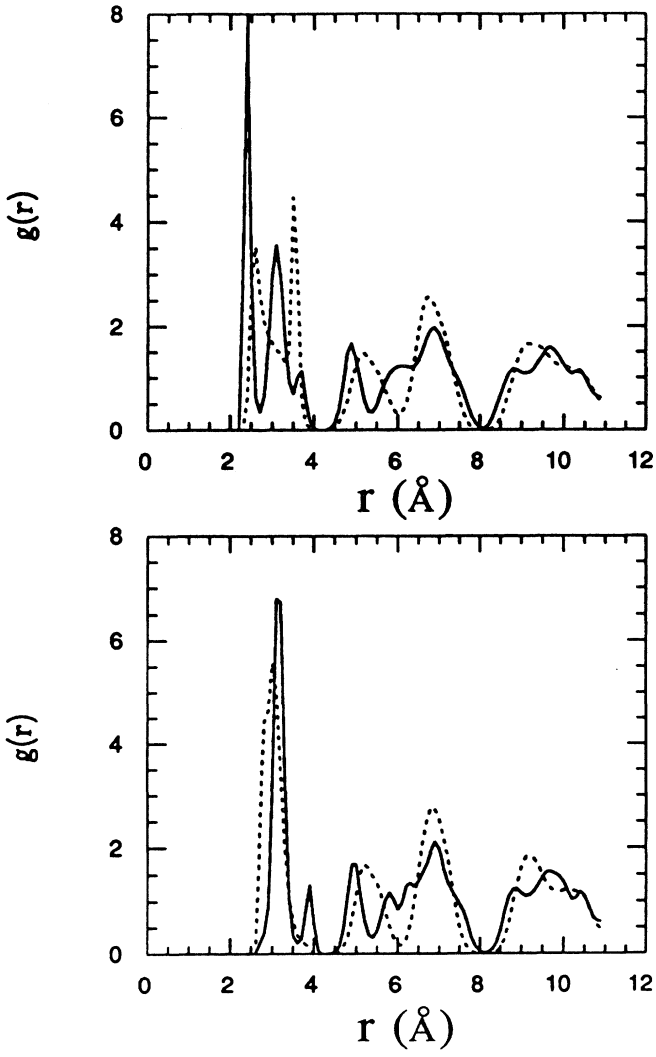

FIG. 7. Pair-distribution functions $g(r)$ for $(NaCN)_{0.5}(KCN)_{0.5}$ at 50 K. Top: Na-C (solid line) and Na-N (dashed line). Bottom: K-C (solid line) and K-N (dashed line).

the cell lengths L_a, L_b, and L_c are equal (within the resolution of the simulations) at each temperature, the cell angles α, β, and γ depart, by about 6° at low temperature, from the perfect cubic angle of 90°. Thus, the simulation cell becomes rhombohedral. The onset of this distortion takes place at about 100 K. The behavior contrasts sharply with that observed in the $x=0.5$ mixture, where the cell remained cubic at all temperatures (Fig. 1).

The variation of the Kubic-harmonics coefficients with temperature is shown in Fig. 11. The relatively large positive values of C_4 and C_6 (0.24 and 0.10, respectively) at 220 K indicate that, even at such a high temperature, in comparison with ~70 K (see Fig. 4), the complete orientational freezing temperature, CN^- ions favor $\langle 100 \rangle$ alignment. This is also clear from the order parameters, displayed in Fig. 12, which show that E_g ordering is stronger than T_{2g} ordering at 220 K. In fact, the time-averaged configurations at $T=220$ K shown in Fig. 13 provide striking evidence for the role played by Na^+ ions in determining the orientations of neighboring CN^- molecules.

Because the disparity in the relative concentrations of cations is large in $(NaCN)_{0.15}(KCN)_{0.85}$ mixtures, the orientational behavior of given CN^- ions depends critically on the identity of its nearest-neighbor cations. For the purpose of the analysis, we divide anions into two groups: those which have *at least one* Na^+ nearest neighbor, and the rest. Two angles, θ and ϕ, the polar and azimuthal angles, respectively, are used to describe the orientation of the linear CN^- ion in spherical coordinates, i.e., $\hat{u}=(\theta,\phi)$ with the z axis of the crystal chosen as the reference for the polar angle. The distribution function of the angles θ and ϕ have been calculated separately for the two types of CN^- ions mentioned above. For convenience, the distributions for the two groups are denoted $\rho_{Na}(\theta)$, $\rho_{Na}(\phi)$, $\rho_K(\theta)$, and $\rho_K(\phi)$. The results for the system at 250 K are plotted in Fig. 14. Clearly, those CN^- ions close to Na^+ (first group) favor $\langle 100 \rangle$ direc-

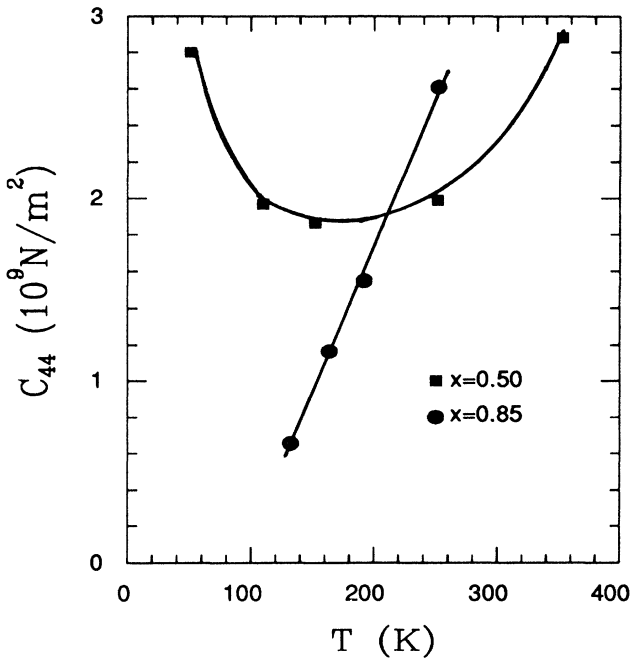

FIG. 9. Temperature dependence of the shear elastic constant c_{44}. For the $x=0.5$ mixture (squares), c_{44} is relatively weakly temperature dependent compared to the $x=0.85$ mixture (solid circles), which exhibits dramatic softening. Since the lattice undergoes a rhombohedral distortion below 90 K, c_{44} is not estimated in that region; it likely has a minimum between 90 and 110 K.

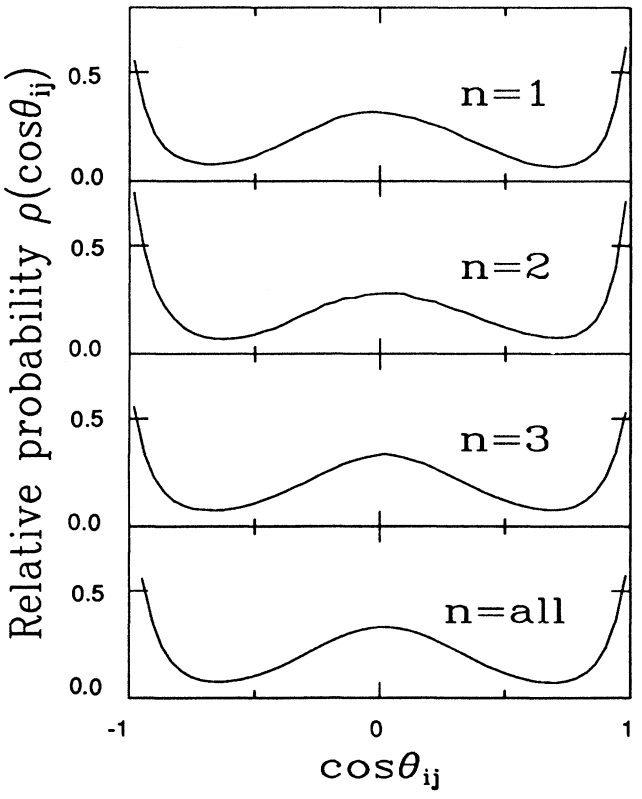

FIG. 8. Probability distribution of angular correlations between bond vectors of pairs of CN^- molecules at 90 K, $\langle \hat{u}_i \cdot \hat{u}_h \rangle = \langle \cos(\theta_{ij}) \rangle$, as a function neighbor shell number, n.

TABLE IV. Thermodynamic properties of the $x=0.85$ mixture. $\langle U_{conf} \rangle$ and $\langle V \rangle$ are the run-averaged configurational energy and volume, respectively.

T (K)	$\langle U_{conf} \rangle$ (kJ mol−1)	$\langle V \rangle$ (Å^3)
50.0	−706.16	257.04
71.8	−705.34	257.73
91.7	−704.48	258.29
111.6	−703.63	259.05
132.1	−702.74	259.93
163.8	−701.46	261.15
191.9	−700.43	262.23
225.8	−699.26	263.55
251.8	−698.29	264.60

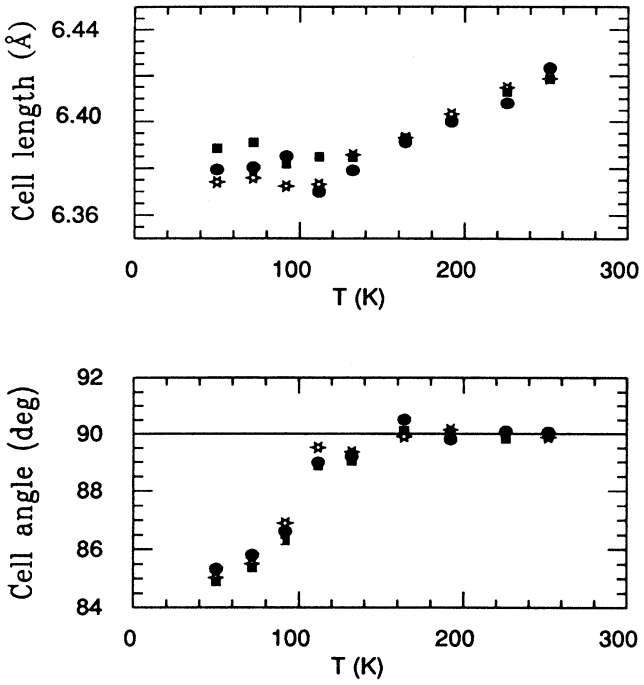

FIG. 10. Same as Fig. 1, but for $x = 0.85$.

tions, while the others (second group) have no preferred orientations. In another words, anions which have a Na^+ neighbor are strongly hindered in their orientational movements, even at high temperatures, while other anions undergo quasifree rotational diffusion. Thus, Na^+ ions play the role of nucleation centers which tend to lock neighboring CN^- molecules into ⟨100⟩ directions.

Unlike $(NaCN)_{0.5}(KCN)_{0.5}$ mixtures, where the ⟨100⟩ orientation definitely dominates, strong competition

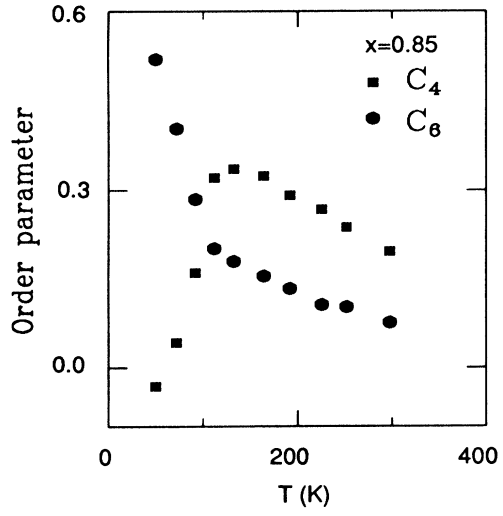

FIG. 11. Same as Fig. 3, but for $(NaCN)_{0.15}(KCN)_{0.85}$.

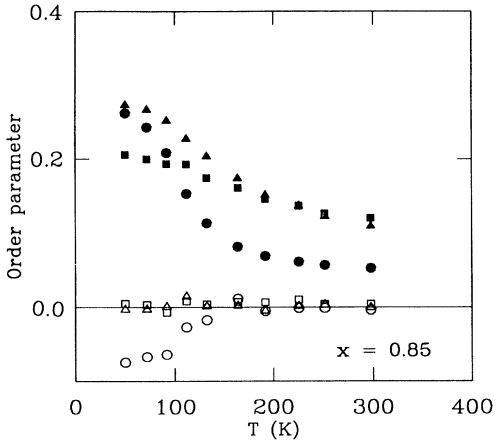

FIG. 12. Same as Fig. 5, but for the $x = 0.85$ mixture.

exists between ⟨100⟩ and ⟨111⟩ ordering in $(NaCN)_{0.15}(KCN)_{0.85}$. This can be seen from the temperature dependence of C_4 and C_6 in Fig. 11. For $(NaCN)_{0.15}(KCN)_{0.85}$, as we have just discussed, the preferred high-temperature orientation is clearly ⟨100⟩. As cooling proceeds, C_4 gradually increases and CN^- freezing sets in. The "amount of freezing" can be approximately quantified by counting the number of CN^- molecules which are librating within a cone of 30° of a particular direction. This number is plotted in Fig. 15 as a function of temperature. The plot reveals the existence of two freezing mechanisms, corresponding to the two groups defined earlier. Thus, the presence of a near-neighbor Na^+ ion will result in ⟨100⟩ locking of a CN^- molecule, while other molecules, whose energetics is dominated by

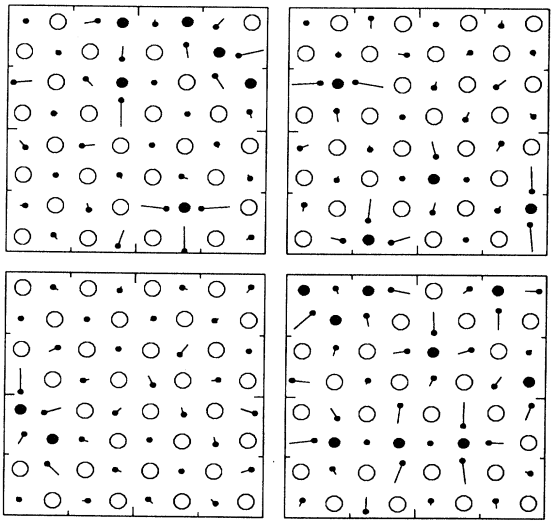

FIG. 13. Same as Fig. 6, but for $(NaCN)_{0.15}(KCN)_{0.85}$ at 220 K. Some CN^- undergo rotational diffusion, while others are locked into ⟨100⟩ directions by neighboring Na^+ ions, causing overall ⟨100⟩ ordering to dominate.

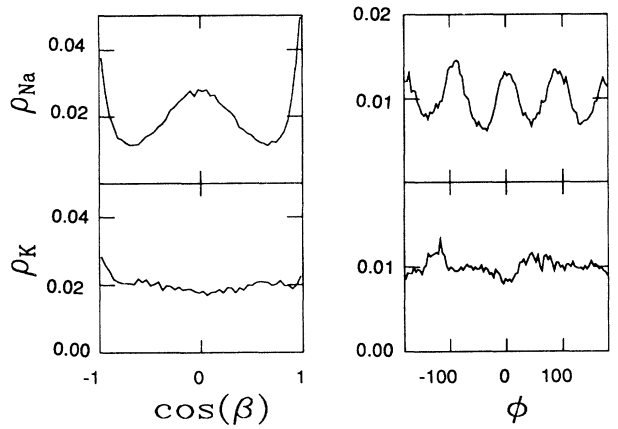

FIG. 14. Distributions of polar (θ) and azimuthal (ϕ) angles for the two groups of CN^- ions discussed in the text, for $(NaCN)_{0.15}(KCN)_{0.85}$ at 220 K. The upper curves (denoted ρ_{Na}) correspond to those CN^- ions that have at least one Na^+ ion nearest neighbor, while the lower curves (denoted ρ_K) are for those CN^- ions that do not.

translation-rotation coupling, will freeze into ⟨111⟩ orientations. The freezing-in temperature (~100 K) of the latter process coincides with the tendency for the lattice to shear. Freezing into ⟨100⟩ begins at a higher temperature in comparison with the initiation of ⟨111⟩ freezing (~140 K), indicated by the increase of

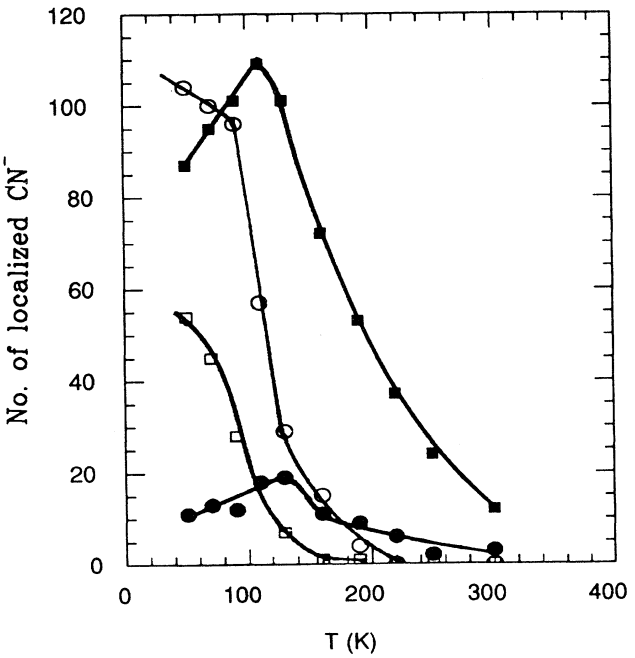

FIG. 15. Number of CN^- ions remaining within a cone of 30° about their mean orientations, as a function of temperature, for the $x=0.85$ mixture. Solid symbols correspond to those preferring ⟨100⟩ pockets, and open symbols to those with ⟨111⟩ orientations. Squares are for CN^- ions *with* at least one Na^+ nearest-neighbor, and circles for CN^- ions *without* any Na^+ nearest-neighbor.

$([\langle Y_{T_{2g}}(\hat{u})\rangle^2]_{av})^{1/2}$ (see below). Correspondingly, ⟨111⟩ freezing causes C_4 to drop dramatically after an initial increase and C_6 to increase rapidly (see Fig. 11). Since ⟨111⟩ freezing dominates over the existing ⟨100⟩ ordering, softening of c_{44} prevails as the temperature decreases.

The competition between the two mechanisms is also visible in the Edwards-Anderson order parameters (Fig. 12). At high temperature, $([\langle Y_{E_g}(\hat{u})\rangle^2]_{av})^{1/2}$ is larger than $([\langle Y_{T_{2g}}(\hat{u})\rangle^2]_{av})^{1/2}$, but the order is reserved below 100 K. Even though those CN^- close to Na^+ are strongly disturbed by the desire to freeze into ⟨111⟩ orientations at low temperatures, as demonstrated by the anomalous shape of the azimuthal angle distribution $\rho_{Na}(\phi)$ at 50 K, Fig. 16, they strive to remain in their local ⟨100⟩ pocket. Figure 15 indicates that 38% of the CN^- that *do* have at least one Na^+ neighbor are, in fact, aligned along ⟨111⟩—rather than ⟨100⟩—at 50 K. The effect is perhaps more clearly demonstrated by the time-averaged configurations displayed in Fig. 17. Here, though, the ⟨100⟩ ordering is evident, most CN^- molecules exhibit a slight tilt away from ⟨100⟩. Regardless of their cation neighbors, 158 out of 256 CN^{-1} ions orient along ⟨111⟩, while others are locked into ⟨100⟩. The small negative value of C_4 at the low temperature results from a combination of ⟨111⟩ and ⟨100⟩ orientational distributions. In the $x=0.85$ mixture, the random strains are weaker than in the $x=0.5$ mixture, and there exists a strong competition between random-strain-orientation and translation-orientation couplings. It is the latter which causes the softening of the T_{2g} mode, as can be seen from the temperature dependence of c_{44} shown in Fig. 9.

IV. DISCUSSION

It is quite remarkable that experimentally it suffices to include only 10% of Na^+ ions in place of K^+ on the cation sublattice in order to suppress the first-order transition which takes place in pure KCN. Because of the large size disparity between Na^+ and K^+, the random strain fields are much larger here than in other

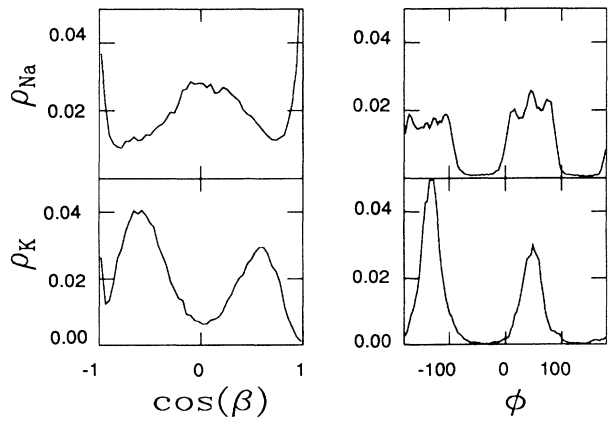

FIG. 16. Same as Fig. 14, but at 50 K.

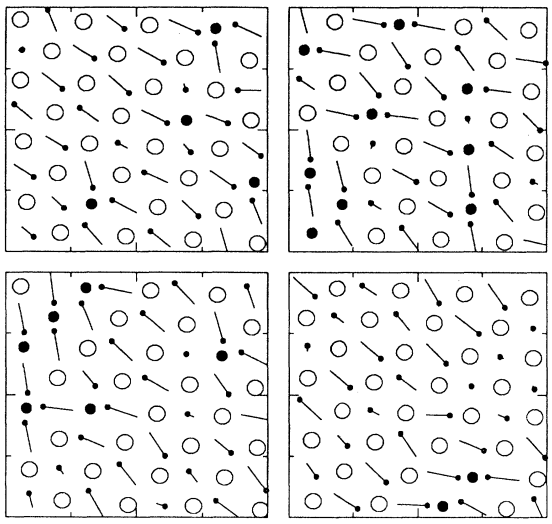

FIG. 17. Same as Fig. 6, but for $x=0.85$ at 50 K. Even though they clearly prefer to stay in the ⟨100⟩ direction, the orientations of those CN^- ions neighboring a Na^+ are perturbed by the rhombohedral distortion and the overall ⟨111⟩ alignment of the anions.

cyanides.[37] This most likely explains why the orientational glass forms over such a wide concentration range.

The present computer-simulation study clearly demonstrates the importance of random strain fields on the low-temperature orientations of the CN^- molecular ions in the mixed cyanides. The effect is particularly strong in $(NaCN)_{1-x}(KCN)_x$ compared to other cyanides: substitution of K^+ by the smaller Na^+ critically lowers the potential minimum in the ⟨100⟩ direction of the orientational energy surface, in which neighboring CN^- ions can then get trapped. In addition, the more electronegative C atoms prefer the proximity of Na^+ ions, because of the stronger electrostatic field produced by the smaller cations. The energetics of the problem thus results in sodium ions acting as nucleation centers which lock near-neighbor CN^- ions into ⟨100⟩ directions; the remaining molecules freeze into ⟨111⟩ pockets. For the $x=0.5$ mixture, where virtually *all* anions have at least one Na^+ neighbor, most CN^- ions are locked into ⟨100⟩ directions randomly. However, at a lower sodium concentration, $x=0.85$, ⟨111⟩ orientations dominate, as only about 38% of the molecules are able to maintain ⟨100⟩ ordering. Competition between the two freezing mechanisms is responsible for an anomalous temperature dependence of the order parameter C_4 which should be seen in experiment.

Predominant freezing into ⟨111⟩ orientations for the low-sodium concentration system results in a substantial rhombohedral distortion of the MD sample—the three angles are sheared by about 6° at low temperature. X-ray-diffraction measurements[11] on a system with the same concentration show no evidence of a structural transition. Instead, the diffraction peaks become broad as temperature decreases which, the authors suggest, is due to significant displacements of the cations from their average cubic sites. Our simulations may not be entirely inconsistent with this result. One possibility is that, for a macroscopic sample, due to a strong competition between the different CN^- orientation ordering mechanisms, local regions form, each distorted to different extents from the ideal cubic symmetry, with correspondingly different spatial orientations for their rhombohedral axes. Thus, on average, the sample remains cubic, and the diffraction peaks suffer broadening. The present calculations were carried out on a rather small system, which can effectively accommodate only one of these "local regions." Of course, a more likely reason for the discrepancy with experiment could be related to an inadequate potential model, which results in different critical concentrations for the phase boundaries between the cubic and distorted phases. Thus, the simulation system of $x=0.85$ may be in the two-phase coexistence region, which is observed experimentally in the concentration range $0.90<x<0.93$, where both cubic and rhombohedral phases are present.[6] The prediction of the exact location of a phase boundary is a stringent test of any potential model and the concomitant simulation technique. In the present case, the overall performance of the potential is satisfactory, given the restrictions of pairwise additive rigid-ion models. In fact, the calculated room-temperature orientational order parameter C_4 (see Fig. 18) agrees rather well with neutron-diffraction data over a wide concentration range. Additional experimental data and further calculations would likely be informative.

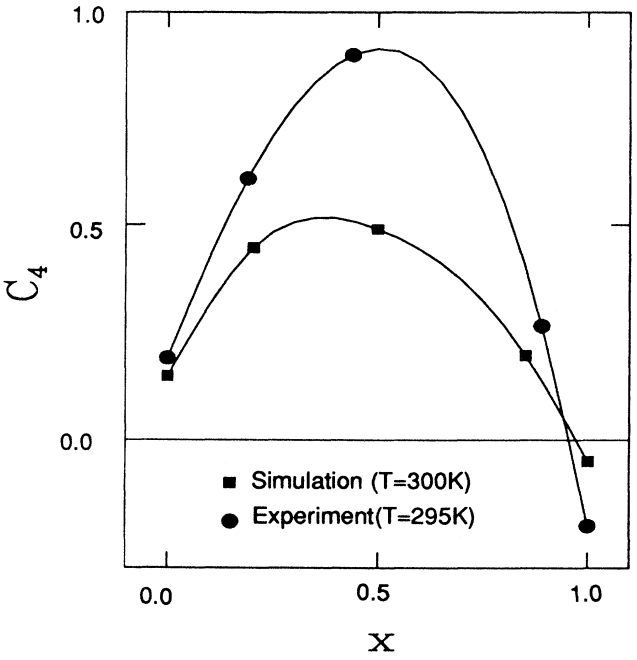

FIG. 18. Concentration dependence of C_4, the first coefficient of the Kubic-harmonics expansion of $f(\hat{u})$ at $T=300$ K. Squares are the present simulation results and circles experimental data for $T=295$ K taken from Refs. 2, 17, and 20.

ACKNOWLEDGMENTS

We thank Dr. Berret, Dr. Böhmer, Dr. Conradi, Dr. Galam, Dr. Knorr, and Dr. Loidl for several illuminating discussions and for sending us details of their unpublished work. This research was supported by the National Science Foundation and by the Natural Sciences and Engineering Research Council of Canada.

[1]F. Lüty, in *Defects in Insulating Crystals,* edited by V. M. Tuchkevich and K. K. Shvarts (Springer-Verlag, Berlin, 1981), p. 69.
[2]J. M Rowe, D. G. Hinks, D. L. Price, S. Susman, and J. J. Rush, J. Chem. Phys. **58**, 2039 (1973).
[3]J. M. Rowe, J. J. Rush, and E. Prince, J. Chem. Phys. **66**, 5147 (1977).
[4]J. M. Rowe, J. J. Rush, N. J. Chester, K. H. Michel, and J. Naudts, Phys. Rev. Lett. **40**, 455 (1978).
[5]J. M. Rowe and S. Susman, Phys. Rev. B **29**, 4727 (1984).
[6]T. Schräder, A. Loidl, T. Vogt, and V. Frank, Physica B **156&157**, 195 (1989).
[7]C. W. Garland, J. O. Fossum, and A. Wells, Phys. Rev. B **38**, 5640 (1988).
[8]Z. Hu, C. W. Garland, and A. Wells, Phys. Rev. B **40**, 5757 (1989).
[9]F. Lüty and J. Ortiz-Lopez, Phys. Rev. Lett. **50**, 1289 (1983).
[10]J. Ortiz-Lopez and F. Lüty, Phys. Rev. B **37**, 5461 (1988).
[11]A. Loidl, T. Schräder, R. Böhmer, K. Knorr, J. K. Kjems, and R. Born, Phys. Rev. B **34**, 1238 (1986).
[12]A. Loidl, Annu. Rev. Phys. Chem. **40**, 29 (1989), and references cited therein.
[13]J. F. Berret, A. Farkadi, M. Boissier, and J. Pelous, Phys. Rev. B **39**, 13 451 (1989).
[14]J. F. Berret and R. Feile, Z. Phys. B **80**, 203 (1990).
[15] J. M. Rowe, J. J. Rush, D. G. Hinks, and S. Susman, Phys. Rev. Lett. **43**, 1158 (1979).
[16]J. M. Rowe, J. J. Rush, and S. Susman, Phys. Rev. B **28**, 3506 (1983).
[17]A. Loidl, K. Knorr, J. M. Rowe, and G. J. McIntyre, Phys. Rev. B **37**, 389 (1988).
[18]A. Loidl, R. Feile, and K. Knorr, Phys. Rev. Lett. **48**, 1263 (1988).
[19]T. Schräder, A. Loidl, and T. Vogt, Phys. Rev. B **39**, 6186 (1989).
[20]T. Schräder, A. Loidl, G. J. McIntyre, and C. M. E. Zeyen, Phys. Rev. B (to be published).
[21]J. H. Walton and M. S. Conradi, Phys. Rev. B **41**, 6234 (1990).
[22]T. Westerhoff and R. Feile (unpublished).
[23]J. Hessinger and K. Knorr, Phys. Rev. Lett. **63**, 2749 (1989).
[24]C. W. Garland, J. Z. Kwiecien, and J. C. Damien, Phys. Rev. B **25**, 5818 (1982).
[25]J. O. Fossum and C. W. Garland, Phys. Rev. Lett. **60**, 592 (1988).
[26]J. O. Fossum and C. W. Garland, J. Chem. Phys. **89**, 7441 (1988).
[27]J. O. Fossum, A. Wells, and C. W. Garland, Phys. Rev. B **38**, 412 (1988).
[28]S. Elschner, K. Knorr, and A. Loidl, Z. Phys. B **61**, 209 (1985).
[29]E. Civera-Garcia, K. Knorr, and A. Loidl, Phys. Rev. B **36**, 8517 (1987).
[30]K. H. Michel and J. M. Rowe, Phys. Rev. B **22**, 1417 (1980).
[31]K. H. Michel, Phys. Rev. Lett. **57**, 2188 (1986).
[32]K. H. Michel, Z. Phys. B **68**, 259 (1987).
[33]C. Bostoen and K. H. Michel, Z. Phys. B **71**, 369 (1988).
[34]K. H. Michel and T. Theuns, Phys. Rev. B **40**, 5761 (1989).
[35]S. Galam, Phys. Lett. A **122**, 271 (1987); J. Appl. Phys. **67**, 5979 (1990); (unpublished).
[36]L. J. Lewis and M. L. Klein, Phys. Rev. Lett. **57**, 2698 (1986); **59**, 1837 (1987).
[37]L. J. Lewis and M. L. Klein, J. Phys. Chem. **91**, 4990 (1987); Phys. Rev. B **40**, 4877 (1989); **40**, 7080 (1989).
[38]M. Parrinello and A. Rahman, Phys. Rev. Lett. **45**, 1196 (1980).
[39]S. Nosé and M. L. Klein, J. Chem. Phys. **78**, 6928 (1983).
[40]S. Nosé and M. L. Klein, Phys. Rev. Lett. **50**, 1207 (1983).
[41]R. W. Impey, S. Nosé, and M. L. Klein, Mol. Phys. **50**, 243 (1983).
[42]R. W. Impey, M. Sprik, and M. L. Klein, J. Chem. Phys. **83**, 3638 (1985).
[43]M. L. Klein, in *Molecular-Dynamics Simulation of Statistical-Mechanical Systems,* Proceedings of the International School of Physics "Enrico Fermi," Course XCVII, 1986, edited by C. Ciccotti and W. G. Hoover (North-Holland, Amsterdam, 1986), p. 424.
[44]D. G. Bounds, M. L. Klein, and I. R. McDonald, Phys. Rev. Lett. **46**, 1682 (1981).
[45]D. G. Bounds, M. L. Klein, I. R. McDonald, and Y. Ozaki, Mol. Phys. **47**, 629 (1982).
[46]M. L. Klein and I. R. McDonald, J. Chem. Phys. **79**, 2333 (1983).
[47]M. Ferrario, I. R. McDonald, and M. L. Klein, J. Chem. Phys. **84**, 3975 (1986).
[48]P. W. Fowler and M. L. Klein, J. Chem. Phys. **85**, 3913 (1986).
[49]M. P. Allen and D. J. Tildesley, *Computer Simulation of Liquids* (Clarendon, Oxford, 1987).
[50]C. W. Gear, *Numerical Initial Value Problems in Ordinary Differential Equations* (Prentice-Hall, Englewood Cliffs, NJ, 1971).
[51]W. R. Fehlner and S. H. Vosko, Can. J. Phys. **54**, 2159 (1976).
[52]S. F. Edwards and P. W. Anderson, J. Phys. F **5**, 965 (1975).